# Ensemble Solar Forecasting Statistical Quantification and Sensitivity Analysis

## Preprint

WanYin Cheung, Jie Zhang, Anthony Florita, and Bri-Mathias Hodge
*National Renewable Energy Laboratory*

Siyuan Lu and Hendrik F. Hamann
*IBM T.J. Watson Research Center*

Qian Sun and Brad Lehman
*Northeastern University*

*Presented at the 5th International Workshop on Integration of Solar Power Into Power Systems*
*Brussels, Belgium*
*October 19–20, 2015*

**NREL is a national laboratory of the U.S. Department of Energy**
**Office of Energy Efficiency & Renewable Energy**
**Operated by the Alliance for Sustainable Energy, LLC**

This report is available at no cost from the National Renewable Energy Laboratory (NREL) at www.nrel.gov/publications.

**Conference Paper**
NREL/CP-5D00-64960
December 2015

Contract No. DE-AC36-08GO28308

**NOTICE**



This report is available at no cost from the National Renewable Energy Laboratory (NREL) at www.nrel.gov/publications.

Available electronically at SciTech Connect http:/www.osti.gov/scitech

Available for a processing fee to U.S. Department of Energy and its contractors, in paper, from:

U.S. Department of Energy
Office of Scientific and Technical Information
P.O. Box 62
Oak Ridge, TN 37831-0062
OSTI http://www.osti.gov
Phone: 865.576.8401
Fax: 865.576.5728
Email: reports@osti.gov

Available for sale to the public, in paper, from:

U.S. Department of Commerce
National Technical Information Service
5301 Shawnee Road
Alexandria, VA 22312
NTIS http://www.ntis.gov
Phone: 800.553.6847 or 703.605.6000
Fax: 703.605.6900
Email: orders@ntis.gov

*Cover Photos by Dennis Schroeder: (left to right) NREL 26173, NREL 18302, NREL 19758, NREL 29642, NREL 19795.*

NREL prints on paper that contains recycled content.

# Ensemble Solar Forecasting Statistical Quantification and Sensitivity Analysis

WanYin Cheung, Jie Zhang,
Anthony Florita, Bri-Mathias Hodge
*National Renewable Energy Laboratory Golden, CO, USA*

Siyuan Lu, Hendrik F. Hamann
*IBM T.J. Watson Research Center Yorktown Heights, NY, USA*

Qian Sun, Brad Lehman
*Northeastern University Boston, MA, USA*

***Abstract*—Uncertainties associated with solar forecasts present challenges to maintain grid reliability, especially at high solar penetrations. This study aims to quantify the errors associated with the day-ahead solar forecast parameters and the theoretical solar power output for a 51-kW solar power plant in a utility area in the state of Vermont, U.S. Forecasts were generated by three numerical weather prediction (NWP) models—including the Rapid Refresh, the High-Resolution Rapid Refresh, and the North American Model (NAM)—and a machine-learning ensemble model. A photovoltaic (PV) performance model was adopted to calculate theoretical solar power generation using the forecast parameters (e.g., irradiance, cell temperature, and wind speed). Errors of the power outputs were quantified using statistical moments and a suite of metrics, such as the normalized root mean square error (NRMSE). In addition, the PV model's sensitivity to different forecast parameters was quantified and analyzed. Results showed that the ensemble model yielded forecasts in all parameters with the smallest NRMSE. The NRMSE of the solar irradiance forecasts of the ensemble NWP model was reduced by 28.10% compared to the best of the three NWP models. Further, the sensitivity analysis indicated that the errors of the forecasted cell temperature attributed only approximately 0.12% to the NRMSE of the power output as opposed to 7.44% from the forecasted solar irradiance.**

***Keywords-solar forecasting; uncertainty; numerical weather prediction; machine learning; sensitivity analysis***

## I. INTRODUCTION

Solar power installation has accelerated rapidly in the United States due to the establishment of state renewable portfolio standards and the decreasing price of photovoltaic (PV) system components [1]. Solar power has been predicted to provide 14% of the U.S. electricity needs by 2030 and 27% by 2050 [2]. However, the uncertainty and variability of solar power create challenges for grid operators to manage the increasing integration of solar power while ensuring continued grid reliability. Thus, solar power forecasting is important in different operating time frames from real time to years to proactively integrate solar power. Longer range forecasts at time horizons beyond weeks ahead help with operation management and planning, maintenance planning, etc. Day-ahead forecasts are useful for unit commitment planning and scheduling of slow-starting thermal units to ensure the balance between generation and anticipated load. Operating schedules are adjusted as they get closer to real time to account for minutes- to hours-ahead forecasts. Forecasts are valuable to assist operators in managing power system reliability and to improve economic efficiency [3-4]. However, forecast inaccuracies can result in issues in power system scheduling, which may lead to significant economic consequences [5]. In addition to improving the accuracy of forecasts, it is critical to better understand the uncertainties inherent in solar power forecasts.

### A. Overview of Solar Forecasting

Different forecasting methods have been developed to forecast solar irradiance and power at time horizons of minutes, hours, and days ahead, including physical-based, statistical-based, and hybrid approaches. The physical approaches, such as cloud movement tracking and numerical weather prediction (NWP) models, rely on weather forecasts and solar panel specifications to generate solar power forecasts [6-8].Short-term irradiance forecasts, based on cloud formation using satellite and ground observation, range from 3 minutes up to 6 hours ahead of the operating point [9]. For forecast horizons beyond 6 hours, NWP models tend to outperform the cloud-movement-based forecasts [10]. Further, ensembles of individual NWP forecasts using machine-learning techniques have been shown to have better accuracies than individual forecasts [11]. NWP models are generally used in conjunction with PV performance simulation tools, such as PV Lib and PVWatts [12-13], to convert harvested solar irradiance to solar power. Statistical approaches, such as regressive modeling and artificial neural networks (ANNs) [14-15], yield power forecasts based on historical data and exogenous variables at time horizons ranging from 5 minutes up to 6 hours [16]. Hybrid forecast methods, such as inputting processed satellite images to ANNs [17] and utilizing model output statistics for ensemble NWP forecasts [18], combine both physical- and statistical- based approaches to yield enhanced forecasts.

### B. Research Objectives

This research aims to better understand the day-ahead solar forecasting errors of three regional NWP models and an ensemble machine-learning model through statistical

quantification and to compare their relative performances. The three studied NWP models are the Rapid Refresh (RAP), the High-Resolution Rapid Refresh (HRRR), and the North America Model (NAM). The PV Lib tool was used to calculate the theoretical solar power generation using the forecasted parameters as inputs [12]. Error statistics of meteorological parameters and solar power were examined at a 51-kW solar power plant in a utility area in Vermont, United States. The sensitivity of the power output to each forecast parameter was also studied to determine the critical parameters in solar forecasting.

The remainder of the paper is organized as follows. Section II summarizes the forecast models and methods used in this study. The results and discussion are presented in Section III. The conclusion and suggestions for future research are included in the final section.

## II. Data and Methods

### A. NWP Models and Ensemble Machine-Learning Model

Regional NWP models—such as RAP, HRRR, and NAM—forecast the atmospheric state based on initial conditions defined by the global NWP models and vertical atmospheric profile. The three studied regional models forecast the atmospheric state at different resolutions and time horizons, as shown in Table I [11]. Because of the coarse-graining of the physical atmospheric state, the regional NWP forecasts often have errors dependent on the current weather situation category. To enhance the accuracy of solar forecasts, the ensemble forecasting model, named Watt-Sun [11, 19], was developed by IBM in collaboration with the National Renewable Energy Laboratory, Argonne, Northeastern University, and others as part of the project work performed under the U.S. Department of Energy's SunShot Initiative for Improving the Accuracy of Solar Forecasting [20]. The ensemble forecasts leverage a machine-learning-based approach to account for categorization parameters— cloud liquid water, ice contents, etc.—in addition to the parameters of direct interests, such as solar irradiance and temperature. The categorization parameters create specific weather categories exhibiting the condition-dependent errors in each model. Thus, the machine-learning model is trained using both sets of parameters from multiple regional models and measurements of prediction parameters to yield improved forecasts [11]. Forecasts generated by both the ensemble model and the individual NWP models were examined in this study.

TABLE I. Resolution and Forecasting Horizon of the NWP Models

| Model | Spatial Resolution and Coverage | Temporal Resolution | Forecasting Horizon |
|---|---|---|---|
| RAP | 13 km | 15 min 2-Dimension<br>1 h 3-Dimension | 18 h |
| HRRR | 3 km | 15 min 2-Dimension<br>1 h 3-Dimension | 15 h |
| NAM | 5 km | 1 h | 0-60 h |

### B. PV Performance Model

The PV performance model PV Lib was adopted in this study to convert available solar irradiance to PV AC power generation at a specific location. Forecasts parameters (e.g., irradiance, cell temperature) generated from the NWP models and the ensemble model were used as the two major inputs to yield power generation. The first variable was effective irradiance, which refers to the total amount of plane of array (POA) irradiance adjusted for the angle of incidence losses, soiling, and spectral mismatch. An assumption of moderate, cleaned PV arrays with 2% irradiance loss was made [21]. Other than directly forecasted cell temperature, the cell temperature can also be calculated in PV Lib based on module materials, incident irradiance, ambient temperature, and wind speed at 10 m. More details about the PV Lib model can be found in [12].

### C. Data Summary

Hourly solar forecasts from the NWP models and the ensemble model of a 51-kW solar power plant were analyzed. Forecast parameters included POA irradiance, solar irradiance components (direct normal irradiance [DNI], diffuse horizontal irradiance [DHI], and global horizontal irradiance [GHI]), ambient temperature ($T_A$), cell temperature ($T_C$), and wind speed (WS). Measurements of four parameters were taken hourly at the site. Hourly data was available from 7 a.m. to 10 p.m. between July 2013 and February 2014. Parameters available from measurements and different models were marked with "+" and are shown in Table II. In this study, to minimize bias errors introduced by relatively small irradiance values, hourly data with measured irradiance less than the threshold irradiance of 5 W/m$^2$ were removed [22].

### D. Statistical Metrics

Three types of errors are present in the process of solar forecasts, including measurement errors due to the measuring devices for different parameters; forecast errors; and irradiance-to-power model errors. In this study, measurement errors were assumed to be negligible due to the limited information about the measurement device. The forecast errors and the model errors were the major focus of this study.

This section presents the statistical metrics used to quantify the forecast errors associated with the parameters and power outputs. The accuracy of the major forecasted inputs and power outputs was determined by comparing them to the measurements. The associated errors were defined as forecast values minus measurement. A suite of metrics were proposed in [23] to evaluate the performance of solar forecasts. In this paper, the errors were characterized by four statistical moments: mean, variance, skewness, and kurtosis. In addition, the 1$^{st}$ order error measurement, mean absolute error (MAE), and the 2$^{nd}$ order error measurement, root mean square error (RMSE), were used to quantify the forecast errors. RMSE provides an overall error measure throughout the forecasting period while weighing heavily on the extreme forecast errors, whereas MAE provides an overall error measure without punishing the extreme forecast-errors [23, 24]. Normalized root mean square error percentages (NRMSE [%]) and normalized mean absolute error percentages (NMAE [%]) were also calculated to compare performances among the four models. Forecast errors of each parameter and power output were normalized by the corresponding capacity

values, i.e., 1,000 W/m$^2$ for irradiance, 19.54°C based on the average measured cell temperature, and 51 kW for the analyzed solar power plant.

Wind speed is also an input of the PV Lib model. A power law was used to estimate the measured wind speed at 10 m, assuming that the solar power plant location has neutral atmospheric conditions:

$$WS_{10} = WS_2 \times \left(\frac{Z_{10}}{Z_2}\right)^{\frac{1}{7}} \quad (1)$$

where $Z$ is the elevation (m) [25].

To analyze and compare the forecast errors at different cloudy conditions, the daily average cloudy conditions were characterized by using the daily average clearness index ($k*$), which is the ratio of the forecasted (or measured) irradiance to the irradiance from the clear-sky model [26]. Based on the daily average clearness index, data were then categorized into different cloud conditions [27], as shown in Table III.

TABLE II. AVAILABLE PARAMETERS FROM DIFFERENT MODELS AND MEASUREMENT

| Parameters | Measure-ment | RAP | HRRR | NAM | Ense-mble |
|---|---|---|---|---|---|
| AC Power (W) | + | | | | |
| POA (W/m$^2$) | + | + | + | + | + |
| GHI (W/m$^2$) | | + | + | + | |
| DNI (W/m$^2$) | | + | + | + | |
| DHI (W/m$^2$) | | + | + | + | |
| $T_C$ (°C) | + | + | + | + | + |
| $T_A$ (°C) | | + | + | + | |
| $WS_2$ (m/s) | + | | | | + |
| $WS_{10}$ (m/s) | | + | + | + | |

TABLE III. CLEARNESS INDEX CATEGORIZATION

| Clearness Index (k*) | Cloud Conditions Category |
|---|---|
| $k* \leq 0.3$ | Overcast |
| $0.3 < k* \leq 0.7$ | Mostly cloudy |
| $0.7 < k* \leq 1$ | Partly cloudy |
| $k* > 1$ | Sunny |

### E. Sensitivity Analysis

Theoretical power generation was computed using the PV Lib. A design of experiments was applied to generate a total of 13 scenarios based on the inputs extracted from the measurements and the forecast models, as shown in Table IV. Through comparisons of outputs from different scenarios in the sensitivity analysis, the errors of the power outputs were investigated to pinpoint the inputs that had a larger influence on the power output and to evaluate the forecast models' performances. Identifying the critical parameters could allocate necessary efforts to reduce forecast errors associated with the specific parameters.

At the beginning of the sensitivity analysis, systematic errors attributed by the PV Lib model were quantified by inputting both measured *POA* and measured $T_c$ in scenario A1. Systematic errors calculated in A1 were later used to subtract from the errors calculated in the following case studies as a way to account for the model error. The first case study focused on examining the sensitivity of power outputs to irradiance compared to cell temperature in the ensemble model. Errors associated with power outputs based on both measured and forecasted inputs of effective irradiance and cell temperature from the ensemble model were compared in scenarios B1-3. The second case study compared the performance of the power outputs among individual forecast models to the ensemble model. Forecasted parameters from each model were used to convert to solar power in scenarios B-, C-, D-, and E-1. The third case study investigated the effects of individual solar irradiance components and *POA* irradiance on calculated cell temperature and on power forecasts in each NWP model in scenarios C-, D-, E-1, C-, D-, E-2 and C-, D-, E-3. Through the sensitivity analysis, optimal combinations of forecast inputs were identified to yield more accurate power forecasts.

TABLE IV. SCENARIOS SIMULATED IN THE PV LIB MODEL

| Scenarios | Input 1-Effective Irradiance | Input 2 – Cell Temperature |
|---|---|---|
| *Measurement* | | |
| A1 | Measured *POA* | Measured $T_C$ |
| *Ensemble Model* | | |
| B1 | Forecasted *POA* | Forecasted $T_C$ |
| B2 | Measured *POA* | Forecasted $T_C$ |
| B3 | Forecasted *POA* | Measured $T_C$ |
| *RAP, HRRR, NAM* | | |
| C, D, E1 | Forecasted *POA* | Forecasted $T_C$ |
| C, D, E2 | Forecasted *POA* | Calculated cell temperature ($T_{C,C}$) based on forecasted $POA$ & $T_A$ & $WS_{10}$ |
| C, D, E3 | Forecasted *POA* | Calculated cell temperature ($T_{C,C}$) based on forecasted $GHI, DNI, and\ DHI$ & $T_A$ & $WS_{10}$ |

## III. RESULTS AND DISCUSSION

### A. Error Quantification of Forecast Parameters

This section presents the forecast errors associated with the POA irradiance, $T_C$, and $WS_{10}$. Table V shows that the ensemble model forecasts had the smallest errors in all forecast parameters. The RMSE of the POA forecast from RAP, HRRR, NAM was 240.88, 275.42, and 254.59 $W/m^2$, respectively. The RMSE of the ensemble POA forecast using the machine-learning approach based on additional categorization parameters was 173.18 $W/m^2$, which is an approximate 28.10% error reduction compared to the best of the individual model. Similarly, the ensemble forecast in cell temperature and wind speed also enabled error reductions better than the best of the individual NWP.

In correlating the error statistics of the irradiance forecasts and the clearness index distribution in Fig. 1, the ensemble model was found to have the largest number of days with correct forecasted cloud conditions, as shown in Table VI. Forecast models were found to predict accurate cloud conditions most often on sunny days. However, because of the use of POA irradiance instead of GHI, the predictions of the cloud structure in a larger spatial area might be limited.

The performance of the forecasts of different parameters was sensitive to the NWP models. The NRMSE (%) of the POA irradiance forecasts generated by the RAP was the smallest, which was approximately 24.09%. As for cell temperature forecasts, the NAM had the smallest NRMSE (%), which was approximately 35.79 %. Last, the HRRR had the smallest NRMSE (%) for the $WS_{10}$ forecasts. The observed better forecasts in a specific forecast model could have been caused by the unique spatial and temporal resolutions utilized in each NWP model. It is important to note that these results were observed at the specific studied location, which may not apply to other sites.

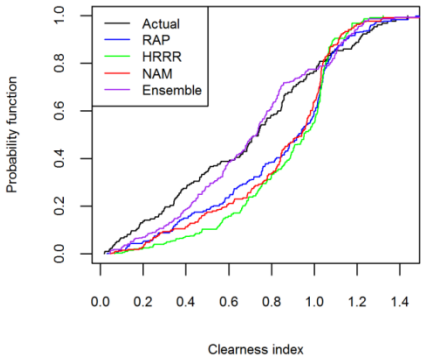


Figure 1. Cumulative distribution of daily clearness index for measurement, three NWP models, and the ensemble model

TABLE V. STASTICAL QUANTIFICATION OF ERRORS ASSOCIATED WITH FORECAST PARAMETERS

| **Plane of Array Irradiance (POA)** | | | | | | | | |
|---|---|---|---|---|---|---|---|---|
| ***Metrics*** | ***Mean ($W/m^2$)*** | ***STD ($W/m^2$)*** | ***Skewness*** | ***Kurtosis*** | ***RMSE ($W/m^2$)*** | ***NRMSE (%)*** | ***MAE ($W/m^2$)*** | ***NMAE (%)*** |
| RAP | 108.70 | 215.02 | 0.71 | 5.26 | 240.88 | 24.09 | 161.51 | 16.15 |
| HRRR | 145.07 | 234.18 | 0.90 | 4.17 | 275.42 | 27.54 | 184.93 | 18.49 |
| NAM | 114.99 | 227.20 | 0.75 | 5.07 | 254.59 | 25.46 | 169.59 | 16.96 |
| Ensemble | -0.94 | 173.23 | 0.18 | 5.17 | 173.18 | 17.32 | 118.54 | 11.85 |
| **Cell Temperature ($T_C$)** | | | | | | | | |
| ***Metrics*** | ***Mean (°C)*** | ***STD (°C)*** | ***Skewness*** | ***Kurtosis*** | ***RMSE (°C)*** | ***NRMSE (%)*** | ***MAE (°C)*** | ***NMAE (%)*** |
| RAP | 4.02 | 6.29 | 0.55 | 4.52 | 7.46 | 38.17 | 5.49 | 28.11 |
| HRRR | 6.08 | 6.46 | 0.77 | 3.94 | 8.87 | 45.38 | 6.72 | 34.39 |
| NAM | 3.14 | 6.26 | 0.37 | 4.29 | 7.00 | 35.79 | 5.17 | 26.46 |
| Ensemble | -0.02 | 4.76 | 0.42 | 4.51 | 4.76 | 24.36 | 3.52 | 17.98 |
| **Wind Speed at 10m ($WS_{10}$)** | | | | | | | | |
| ***Metrics*** | ***Mean (m/s)*** | ***STD (m/s)*** | ***Skewness*** | ***Kurtosis*** | ***RMSE (m/s)*** | ***MAE (m/s)*** | | |
| RAP | 1.60 | 1.40 | -0.27 | 3.56 | 2.13 | 1.82 | | |
| HRRR | 1.24 | 1.27 | -0.13 | 4.09 | 1.78 | 1.46 | | |
| NAM | 2.34 | 1.70 | 0.15 | 3.42 | 2.89 | 2.47 | | |
| Ensemble | -0.01 | 1.01 | -0.98 | 6.41 | 1.01 | 0.73 | | |

TABLE VI. NUMBER OF DAYS WITH ACCURATE CLOUD CONDITIONS FORECASTS

| **Model** | **Overcast** ($k* \leq 0.3$) | **Mostly Cloudy** ($0.3 < k* \leq 0.7$) | **Partly Cloudy** ($0.7 < k* \leq 1$) | **Sunny** ($k* > 1$) | **Total # of correct days** | **% of accuracy** |
|---|---|---|---|---|---|---|
| Measurement | 37 | 46 | 48 | 33 | 164 | |
| RAP | 19 | 20 | 16 | 27 | 82 | 50.00% |
| HRRR | 10 | 14 | 15 | 26 | 65 | 39.63% |
| NAM | 18 | 15 | 21 | 23 | 77 | 46.95% |
| Ensemble | 24 | 33 | 25 | 23 | 105 | 64.02% |

### *B. Systematic Errors in the Conversion Model*

Systematic errors of the PV Lib model were first quantified based on the measured POA irradiance and measured $T_C$ in scenario A1. The measurement errors were assumed to be negligible because of limited information, and thus errors obtained in scenario A1 were assumed to be attributed by the PV Lib model. The PV Lib model was found to have a strong tendency to overpredict, as shown in the positive mean in scenario A1 in Table VII. The NRMSE and NMAE were found to be 9.55% and 3.83%, respectively, which were used to subtract from the normalized errors associated with the other 12 scenarios.

### *C. Sensitivity Analysis for Inputs in the Ensemble Model*

In analyzing the errors introduced by individual input, the NRMSE attributed by the $T_C$ forecasts (B2) and POA irradiance forecasts (B3) were found to be 0.12 % and 7.44%, respectively, as shown in Table VII. Results illustrated that accurate POA irradiance forecasts were able to improve the power output accuracy in a larger magnitude compared to the $T_C$ forecasts. By changing the input from forecast irradiance in scenario B1 to measured irradiance in scenario B2, the NMAE was reduced by 6.35%. As for scenario B3, by inputting measured cell temperature, the NMAE was reduced only by 0.48%, as observed in Fig. 2.

### D. Performance Comparison Among Models

As shown in Table VII, the power output forecasts yielded by the ensemble model (B1) outperformed the three NWP models (C, D, and E-1). The NRMSE was 6.63% for ensemble forecast compared to 14.04% for RAP, 17.14% for HRRR, and 14.88% for NAM. The NRMSE of the ensemble model had an error reduction of 52.83% compared to the best individual NWP model.

The distribution of the power errors of each model is shown in Fig. 3. The positive error tails indicated that all models exhibited an over-forecast tendency. The distribution of errors in the ensemble model was narrower than the other individual NWP models, and it had a larger probability with smaller errors. Among the individual NWPs, the power outputs of RAP were the most accurate, followed by the NAM and the HRRR.

### E. Sensitivity Analysis on Calculated Cell Temperature and Power Output in Individual NWP Models

This section studied whether calculated cell temperature would yield more accurate power forecasts compared to directly forecasted cell temperature. Calculated cell temperature was based on $T_A$, $WS_{10}$, and either POA irradiance (scenario C, D, and E2) or individual solar irradiance components (scenario C, D, and E3). Table VII shows that by changing the forecasted cell temperature in C, D, and E1 to the calculated cell temperature in C, D, and E2 in all three models, the RMSE increased by at most 14 W and the MAE increased by at most 4 W, accounting for less than 0.02% of the site's solar capacity. No improvement in the accuracy of solar power output was observed.

By using calculated cell temperature based on individual solar irradiance components in C, D, and E3, the RMSE was decreased for the RAP but increased for the HRRR and the NAM. In contrary, the NMAE was reduced by 35 W for the RAP and the HRRR and 24 W for the NAM, indicating that the overall errors were reduced by approximately 0.05%.

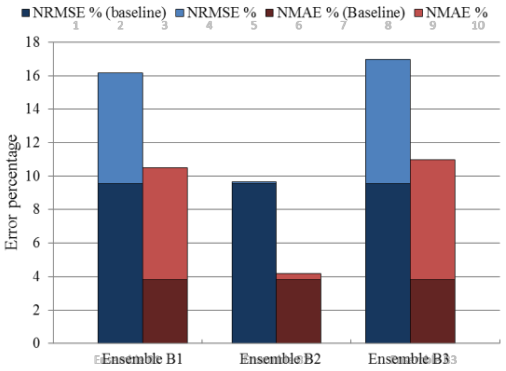


Figure 2. Relative RMSE and MAE percentage for the power outputs in scenarios B1-3 accounting for the systematic errors, which are represented by the darker parts of the bar.

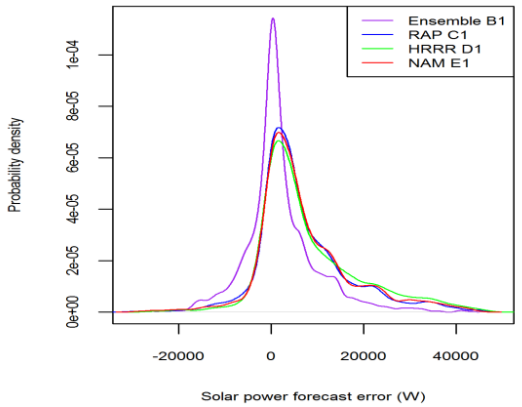


Figure 3. Error distribution of power outputs in scenarios B,C,D, and E1, where all scenarios used forecast POA irradiance and cell temperature.

TABLE VII. STATISTICAL QUANTIFICATION OF POWER ERRORS FOR ALL SCENARIOS

| Metrics | Mean (W) | STD (W) | Skewness | Kurtosis | RMSE (W) | NRMSE (%) | MAE (W) | NMAE (%) |
|---|---|---|---|---|---|---|---|---|
| ***Theoretical Power based on measurement*** | | | | | | | | |
| A1 | 1840.70 | 4508.69 | 6.36 | 53.12 | 4868.82 | 9.55 | 1950.75 | 3.83 |
| ***Ensemble*** | | | | | | | | |
| B1 | 2022.55 | 7997.94 | 1.00 | 6.71 | 3378.78 | 6.63 | 3412.48 | 6.69 |
| B2 | 1973.32 | 4519.16 | 5.93 | 48.34 | 61.26 | 0.12 | 175.75 | 0.34 |
| B3 | 2021.44 | 8424.81 | 1.05 | 6.73 | 3792.88 | 7.44 | 3656.32 | 7.17 |
| ***RAP*** | | | | | | | | |
| C1 | 6642.53 | 10033.71 | 0.98 | 5.13 | 7162.13 | 14.04 | 6257.44 | 12.27 |
| C2 | 6643.67 | 10046.34 | 0.99 | 5.14 | 7173.29 | 14.07 | 6259.45 | 12.27 |
| C3 | 6606.64 | 10055.58 | 1.00 | 5.16 | 7160.62 | 14.04 | 6222.86 | 12.20 |
| ***HRRR*** | | | | | | | | |
| D1 | 8157.81 | 10896.54 | 1.03 | 4.22 | 8740.73 | 17.14 | 7321.67 | 14.36 |
| D2 | 8160.12 | 10912.51 | 1.03 | 4.24 | 8754.90 | 17.17 | 7325.06 | 14.36 |
| D3 | 8125.76 | 10924.18 | 1.04 | 4.25 | 8743.70 | 17.14 | 7286.20 | 14.29 |
| ***NAM*** | | | | | | | | |
| E1 | 7042.59 | 10279.75 | 0.92 | 4.80 | 7589.66 | 14.88 | 6584.63 | 12.91 |
| E2 | 7043.33 | 10287.69 | 0.92 | 4.81 | 7596.63 | 14.90 | 6585.99 | 12.91 |
| E3 | 7019.16 | 10304.64 | 0.93 | 4.82 | 7596.99 | 14.90 | 6560.67 | 12.86 |

## IV. CONCLUSIONS AND FUTURE WORK

This paper characterized and analyzed errors and uncertainties inherent in forecast parameters generated by the three NWP models and the ensemble model. The sensitivity of power output to different forecast parameters was also quantified. The study was applied to a 51-kW solar power plant. Results showed that the ensemble model performed better than the three individual NWP models. Among the three individual NWP models at the studied site, the RAP was able to yield more accurate forecasts in POA irradiance, the HRRR in wind speed, and the NAM in cell temperature.

To analyze the sensitivity of power output to different forecasted solar parameters, a total of 13 scenarios were investigated. Results showed that (i) POA irradiance had a larger influence on the power outputs compared to cell temperature; (ii) all four models presented over-forecast behaviors; and (iii) using the calculated cell temperature instead of directly forecasted cell temperature can slightly increase the overall forecast accuracy of the solar power generation.

Future studies will focus on quantifying uncertainties in forecast parameters for particular seasons or for a longer period of time, as well as for other geographical regions. Further, future sensitivity analyses will attempt to identify an optimal set of forecast parameters that can generate more accurate solar power forecasts.

## ACKNOWLEDGMENT

NREL's contribution to this work was supported by the U.S. Department of Energy under Contract No. DE-AC36-08-GO28308 with the National Renewable Energy Laboratory.

## REFERENCES

[1] G. Klise and J. Stein, Models Used to Assess the Performance of Photovoltaic Systems. Albuquerque, NM: Sandia National Laboratories, 2009.

[2] U.S. Department of Energy SunShot Initiative, Sunshot Vision Study. Washington, D.C.: 2012.

[3] North America Electric Reliability Corporation, Variable Generation Power Forecasting For Operations. New Jersey: N.p., 2010. Print. NERC IVGTF Task 2.1 Report.

[4] GE Energy and Energy Consulting, The Effects of Integrating Wind Power on Transmission System Planning, Reliability, and Operation. Schenectady, NY: 2005. Print.

[5] P. Denholm and R. Margolis, "Evaluating the limits of solar photovoltaics (PV) in traditional electric power systems," Energy Policy, vol. 35, 2007.

[6] C. Chow, B. Urquhart, M. Lave, A. Dominguez, J. Kleissl, J. Shields, and B. Washom, "Intra-hour forecasting with a total sky imager at the UC San Diego solar energy testbed," Solar Energy, vol. 85, 2011.

[7] R. Marquez and C. Coimbra, "Intra-hour DNI forecasting based on cloud tracking image analysis," Solar Energy, vol. 91, 2013.

[8] P. Mathiesen and J. Kleissl, Evaluation of Numerical Weather Prediction for Solar Forecasting. Sacramento: California Energy Commission, 2012.

[9] A. Hammer, D. Heinemann, E. Lorenz, and B. Lückehe, "Short-term forecasting of solar radiation: A statistical approach using satellite data," Solar Energy, vol. 67, 1999.

[10] E. Lorenz, D. Heinemann, H. Wickramarathne, H. Beyer, and S. Bonfinger, "Forecast of ensemble power production by grid-connected PV systems," in 20th European PV Conference, Milano, Italy, 2007.

[11] S. Lu, Y. Huang, I. Khabibrakhmanov, F. Marianno, X. Shao, J. Zhang, B. Hodge, and H. Hamann, "Machine learning based multi-physical-model blending for enhancing renewable forecast-improvement via situation dependent error correction," in European Control Conference, Linz, Austria, July 15-17, 2015.

[12] Sandia National Laboratories, PV Performance Modeling Collaborative. 2015.

[13] National Renewable Energy Laboratory, PVWatts Calculator. 2014.

[14] H. Landsberg, "Solar Radiation at the Earth's surface," Solar Energy, vol. 5, 1961.

[15] B. Amrouche and X. Le Pivert, "Artificial neural network based daily local forecasting for global solar radiation," Applied Energy, vol. 130, pp. 333-341, 2014. Web.

[16] R. Inman, H. Pedro and C. Coimbra, "Solar forecasting methods for renewable energy integration," Progress In Energy and Combustion Science, vo. 39, 2013.

[17] R. Marquez, H.T.C. Pedro, and C.F.M. Coimbra, "Hybrid solar forecasting method uses satellite imaging and ground telemetry as inputs to anns," Solar Energy, vol. 92, pp. 176-188, 2013. Web.

[18] P. Mathiesen and J. Kleissl, "Evaluation of numerical weather prediction for intra-day solar forecasting in the continental United States," Solar Energy, vol. 85, 2011.

[19] U.S. Department of Energy, IBM Thomas J. Watson Research Center, Watt-Sun: A Multi-Scale, Multi-Model, Machine-Learning Solar Forecasting Technology. Washington, D.C., and Yorktown Heights, NY, 2013.

[20] U.S. Department of Energy, Sunshot Initiative: Improving the Accuracy of Solar Forecasting. Washingotn, D.C.: 2012.

[21] Sandia National Laboratories, Photovoltaic Array Performance Model. Albuquerque, NM: N.p., 2004. Print.

[22] T. Hoff, R. Perez, J. Kleissl, D. Renne, and J. Stein, "Reporting of irradiance modeling relative prediction errors," Progress In Photovoltaics: Research And Applications, vol. 21, 2012.

[23] J, Zhang, A. Florita, B.-M Hodge, S. Lu, H. Hamann, V. Banunarayanan, and A. Brockway, "A suite of metrics for assessing the performance of solar power forecasting," Solar Energy, vol. 111, pp. 157-175, 2015. Web.

[24] J, Zhang, A. Florita, B.-M Hodge, S. Lu, H. Hamann, and V. Banunarayanan, "Metrics for evaluating the accuracy of solar power forecasting," in 3rd International Workshop on Integration of Solar Power Into Power Systems, 2013. Print.

[25] J. Newman and P. Klein, "Extrapolation of wind speed data for wind energy applications".

[26] J. Kleissl, Solar Energy Forecasting And Resource Assessment. Academic Press: 2013. Print.

[27] T. McCandless, S. Haupt, and G. Young, ''Short-term solar radiation forecasts using weather regime-dependent artificial intelligence techniques" in American Meteorology Society Conference, 2014.